Validation of the $\mathcal{V}$-index through Finite Element 2D Simulations

Roberto Sassi[1], Luca T Mainardi[2], Pablo Laguna[3,4], Jose F Rodriguez[3,4]

[1] Dipartimento di Informatica, Università degli Studi di Milano, Italy
[2] Dipartimento di Bioingegneria, Politecnico di Milano, Italy
[3] Aragón Institute for Engineering Research (I3A), IIS, University of Zaragoza, Spain
[4] CIBER de Bioingeniería, Biomateriales y Nanomedicina (CIBER-BBN), Zaragoza, Spain

Abstract

A physiological spatial heterogeneity of ventricular repolarization (SHVR) is responsible for the T-wave on the ECG. However, an increased SHVR might favor the development of ventricular arrhythmias. The $\mathcal{V}$-index is a metric introduced with the aim of assessing SHVR from ECG.

In this work, the $\mathcal{V}$-index was validated by means of 2D computer simulations, using a modified version of the ten Tusscher–Panfilov (TP06) model that accounts for repolarization variability. Synthetic ECG were simulated at 12 different positions at the external surface with two different strategies. Also, a theoretical extension of the $\mathcal{V}$-index definition was derived, to address situations where fluctuations in repolarization times are correlated across nodes.

At tissue level, theoretical values of $\mathcal{V}$-index were in agreement with SHVR with a constant pacing (maximum error: 3.4 ms). However, with a variable RR, a selection of stationary beats was necessary to overcome the stronger temporal correlation across nodes (maximum error: 3.2 ms). On the other hand, values of $\mathcal{V}$-index numerically estimated from the ECG were always in agreement with their theoretical values (average error in the estimates: 15±9%). The results confirmed that the $\mathcal{V}$-index indeed provides an approximate and reliable measure of SHVR.

1. Introduction

A specific spatial heterogeneity of ventricular repolarization (SHVR) characterizes the myocardium and it is responsible for the T-wave on the ECG. However, an increased SHVR might favor the development of ventricular arrhythmias.

The $\mathcal{V}$-index is a metric derived from an electrophysiological model [1] and introduced to assess SHVR from ECG. (Please refer to the original paper for a constructive definition). Briefly, under the following hypotheses:

i. the electromagnetical problem is quasi-static;

ii. the inner (c_i) and outer (c_o) domains' conductance tensors have equal anisotropy ratios;

iii. the myocytes' transmembrane potential (TMP) is approximatively similar across different cells, during repolarization (phase 3);

the T–wave on surface ECG, in the kth beat, is given by [2]

$$\mathbf{\Psi}(t) \approx \underbrace{-\mathbf{A}\Delta\boldsymbol{\rho}}_{\boldsymbol{w}_1} \, T_d(t) + \underbrace{\text{1/2}\mathbf{A}\Delta\boldsymbol{\rho}^2}_{\boldsymbol{w}_2} \, \dot{T}_d(t). \qquad (1)$$

Once subdivided the heart in a number M of sources or "nodes" of index m, $\rho_m(k)$ is the repolarization time (*i.e.* the instant where the TMP's first derivative is minimum). Then, $\bar{\rho}(k) = \frac{1}{M}\sum_{m=1}^{M}\rho_m(k)$ is the average repolarization time and $\Delta\rho_m(k) = \rho_m(k) - \bar{\rho}(k)$ the corresponding repolarization delay. In eq. (1), $\Delta\boldsymbol{\rho} = [\Delta\rho_1,\dots,\Delta\rho_M]^T$ and $\Delta\boldsymbol{\rho}^2 = [\Delta\rho_1^2,\dots,\Delta\rho_M^2]^T$. $\mathbf{A}$ is a patient–dependent $[L \times M]$ transfer matrix[1] accounting for the contribution of each node to the L-leads ECG in $\mathbf{\Psi}(t)$. The terms $\boldsymbol{w}_1$ and $\boldsymbol{w}_2$ are $[L \times 1]$ vectors of lead factors (a scalar for each lead), and are prominent in the rest of the paper. The function $T_d(t)$ is shared across leads.

Furthermore [1], adding the two following assumptions:

iv. fluctuations in repolarization times, among successive beats, are modelled as i.i.d. normal random variables, *i.e.* $\varphi_m(k) \sim \mathcal{N}(0,\sigma_{\varphi_m}^2)$ at beat k and also:

   a) φ_m and $\varphi_{n \neq m}$ are uncorrelated across nodes;

   b) $\sigma_{\varphi_m} = \sigma_\varphi$ is constant among nodes and in time;

v. the heart rate is stationary (*i.e.* SDNN [3] is *small enough* in the period under analysis),

and modeling each repolarization delay as

$$\Delta\rho_m(k) = \vartheta_m + \varphi_m(k),$$

where ϑ_m is constant in time, it is also true that, defining an aggregate measure of variability,

$$s_\vartheta = \left(\sum_{m=1}^{M}\frac{\vartheta_m^2}{M}\right)^{1/2} \approx \frac{\text{std}\,[w_2(i)]}{\text{std}\,[w_1(i)]} = \mathcal{V}_i. \qquad (2)$$

---

[1] The matrix $\mathbf{A}$ is constant in time. Clearly, this is only an approximation (*i.e.* it slightly changes due to respiration or other torso movements, myocardial contraction, …), but largely accepted in practice.

For each lead i, the standard deviations (std) are computed, across a certain number of consecutive beats. The term $\mathcal{V}_i$, the so–called $\mathcal{V}$-index, is a measure of SHVR.

In the present work, we will first provide a theoretical formulation of the $\mathcal{V}$-index, when the two hypothesis iv.a) and iv.b) are relaxed. Second, we will validate the metric by means of 2D finite element simulations. These validations are far more demanding in computational terms (and numerically precise) that what done previously in [1, 4], where an equivalent surface source (ESS) model was employed. Finally, employing varying interbeats intervals, we will start to discuss how small SDNN must be in assumption v., so that eq. (2) still holds.

2.   Methods

2.1.   An extension to the $\mathcal{V}$-index definition

Let us relax hypotheses iv.a) and iv.b). First, we suppose that the correlations between fluctuations in repolarization times, $\mathrm{cov}(\varphi_m, \varphi_n) = r(\varphi_m, \varphi_n)$, do not necessarily vanish when $m \neq n$. Also, we assume σ_{φ_m} to vary among nodes. Following [1] and averaging over k, the variances of $w_1(i)$ and $w_2(i)$ are

$$\mathrm{var}\,[w_1(i)] = \sum_{m=1}^{M} \sum_{n=1}^{M} A_{im} A_{in} r\,(\varphi_m, \varphi_n) \tag{3a}$$

$$\mathrm{var}\,[w_2(i)] = \sum_{m=1}^{M} \sum_{n=1}^{M} \frac{A_{im} A_{in}}{4} \mathrm{cov}\,\left(\Delta\rho_m^2, \Delta\rho_n^2\right). \tag{3b}$$

Then, noticing that

$$\mathrm{cov}\,\left(\Delta\rho_m^2, \Delta\rho_n^2\right) = 2\,[r\,(\varphi_m, \varphi_n)]^2 + 4\vartheta_m \vartheta_n r\,(\varphi_m, \varphi_n),$$

equation (3b) becomes

$$\mathrm{var}\,[w_2(i)] = \sum_{m=1}^{M} \sum_{n=1}^{M} \frac{A_{im} A_{in}}{2}\,[r\,(\varphi_m, \varphi_n)]^2$$
$$+ \sum_{m=1}^{M} \sum_{n=1}^{M} A_{im} A_{in} \vartheta_m \vartheta_n r\,(\varphi_m, \varphi_n),$$

or equivalently

$$\mathrm{var}\,[w_2(i)] = \sum_{m=1}^{M} \sum_{n=1}^{M} \frac{A_{im} A_{in}}{2}\,[r\,(\varphi_m, \varphi_n)]^2$$
$$+ s_\vartheta^2 \,\mathrm{var}\,[w_1(i)]$$
$$+ \sum_{m=1}^{M} \sum_{n=1}^{M} \left(\vartheta_m \vartheta_n - s_\vartheta^2\right) A_{im} A_{in} r\,(\varphi_m, \varphi_n).$$

Hence, we have

$$\mathcal{V}_i = \frac{\mathrm{std}\,[w_2(i)]}{\mathrm{std}\,[w_1(i)]} = \sqrt{\mathcal{B}_1 + s_\vartheta^2 + \mathcal{B}_2}, \tag{4}$$
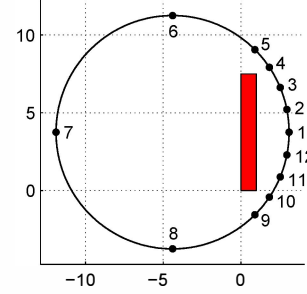

Figure 1.   Geometry employed. Dots mark the positions where the ECG were simulated ("leads").

with

$$\mathcal{B}_1 = \frac{1}{2} \frac{\sum_m \sum_n A_{im} A_{in} \,[r\,(\varphi_m, \varphi_n)]^2}{\sum_m \sum_n A_{im} A_{in} r\,(\varphi_m, \varphi_n)}$$

$$\mathcal{B}_2 = \frac{\sum_m \sum_n \left(\vartheta_m \vartheta_n - s_\vartheta^2\right) A_{im} A_{in} r\,(\varphi_m, \varphi_n)}{\sum_m \sum_n A_{im} A_{in} r\,(\varphi_m, \varphi_n)}.$$

The term $\mathcal{B}_1 \ll s_\vartheta^2$ as long as $\sigma_{\varphi_m} \ll s_\vartheta$, a physiologically reasonable assumption as discussed in [1]. An evaluation of $\mathcal{B}_2$ is not straightforward and analytically challenging. We will numerically evaluate it using the simulations of the next sessions. Clearly, when both terms are small enough, than $\mathcal{V}_i \approx s_\vartheta$ and it still measures SHVR.

2.2.   Finite element 2D forward simulations

A mathematical description of the TMP ϕ_m is given by the bidomain model [5], which is in general difficult to solve and analyze. However, it can be simplified to a single PDE, with assumptions similar to our hypothesis (ii), reducing to the so called monodomain model [6]

$$\nabla \cdot (\bar{c}_i \nabla \phi_m) = C_m \frac{\partial \phi_m}{\partial t} + J_{\mathrm{ion}},$$

which, while adequate for studying heart's variability, simplifies numerical computations. C_m is the cell membrane capacitance, $\bar{c}_i = (1 + \lambda)c_i$ is the effective intracellular conductivity tensor, and λ the ratio between c_o and c_i. Homogeneous Neumann conditions are used at the borders.

For the ionic currents (J_{ion}) we used the tenTusscher–Panfilov (TP06) model [7]. We speculated that fluctuations in ionic currents, caused by stochasticity in ion channels gating, contributes to SHVR. Hence, we modified the Hodking-Huxley formulation for the I_{Ks} gating variable, replacing it with a Langevin stochastic differential equation [8]. In addition, extrinsic noise was included at tissue level, by incorporating cell-to-cell differences in the number of I_{Ks} channels n_{Ks} which was obtained from a log-normal distribution. Further details can be found in [8].

We simulated a vertical slab of "myocardial" tissue, using the following proportion of cells [9]: ENDO 50%,

Table 1. Summary of the results obtained from the synthetic ECG, built: a) solving the diffusion equation (6) in the outer domain (strategy A); b) solving the full (coarser) bidomain problem in the whole domain (strategy B).

	Strategy A				Strategy B			
Case:	**1**	**2**	**3**	**3***	**1**	**2**	**3**	**3***
# beats	200	200	200	41	200	200	200	41
σ_{φ_m} (ms)	0.4	0.3	0.4	0.4	0.3	0.3	0.4	0.4
s_ϑ (ms)	14.5	14.5	14.4	14.5	14.4	14.4	14.3	14.4
$\mathcal{V}$ (ms)	11.1	5.5	7.4	11.3	12.5	4.7	8.8	12.0
$\mathcal{B}_1$ (ms^2)	0.05	0.001	0.04	0.06	0.04	0.001	0.03	0.05
s_ϑ^2 (ms^2)	209.8	209.2	207.4	210.0	206.5	205.8	204.1	206.7
$\mathcal{B}_2$ (ms^2)	-86.6	-179.0	-152.7	-83.9	-50.9	-184.0	-127.4	-64.4
$\widetilde{\mathcal{V}}$ (ms)	14.4	5.5	9.1	13.2	14.4	6.7	10.1	13.0

MID 30% and EPI 20%. A structured grid with square elements was used (size 0.01 cm, 101×751 nodes).

After inserting asymmetrically the slab in a circular volume conductor of diameter 15 cm, synthetic ECG were obtained at 12 different positions ("leads") of the external surface, as in fig. 1. Two sets of ECG were obtained. First (**strategy A**), we integrated over the volume of the slab $\mathcal{H}$

$$\psi = -\int_{\mathcal{H}} \bar{c}_i \nabla \phi_m \cdot \nabla Z \mathrm{d}v, \qquad (5)$$

where ∇Z is the transfer impedance function, relating the current dipole $\bar{c}_i \nabla \phi_m$ in the volume $\mathrm{d}v$ with the potential it generates in the lead. For an infinite homogenous medium surrounding the heart, $Z = c_t^{-1}/(4\pi d)$, being c_t the conductivity of the medium and d the distance between the lead and $\mathrm{d}v$. If $\bar{c}_i$ and c_t are uniform, eq. (5) becomes:

$$\psi = -\frac{c_t^{-1}\bar{c}_i}{4\pi} \int_{\mathcal{H}} \nabla \phi_m \cdot \nabla \left(\frac{1}{d}\right) \mathrm{d}v. \qquad (6)$$

Second (**strategy B**), we solved over the whole domain (the slab and the volume conductor) the full bidomain problem, still under hypothesis (ii), using an unstructured grid of 11161 nodes. To render the computation feasible: (a) the slab was down-sampled to 1013 nodes; (b) the time evolution of the ionic model at each node of the decimated mesh was obtained from interpolation of the high resolution monodomain solution. While approximated, this strategy was proposed in [10] and proved sufficiently precise.

The stimulus, which started each contraction, was given at fixed intervals of 800 ms or at the position of a heart beat, as obtained from Holter ECG records on a healthy patient (mean RR: 772 ms, SDNN: 78 ms). A variable RR sequence was considered to incorporate beat to beat variability, as induced by the autonomous nervous system. A total of 5 minutes for each of the following three **cases** were obtained: **1**) I_{Ks} stochastic gating in the TP06 model and periodic stimuli (375 beats); **2**) no stochastic gating and "variable" stimuli obtained from the real RR series

(392 beats); and **3**) I_{Ks} stochastic gating and variable stimuli. In the followings, numbers label the different cases. When relevant, to specify the computational strategy used for synthetic ECG, a letter is concatenated (*i.e.* 1B).

2.3. $\mathcal{V}$-index estimates

Theoretical values of the lead factors $\boldsymbol{w}_1$ and $\boldsymbol{w}_2$ were computed using the expressions given in eq. (1), with the aid of an exact coupling matrix $\mathbf{A}$ derived from the numerical schemes. Then, $\mathcal{V}$-index's theoretical values ($\mathcal{V}_i$) were obtained with $\mathcal{V}_i = \mathrm{std}[w_2(i)]/\mathrm{std}[w_1(i)]$.

The lead factors $\boldsymbol{w}_1$ and $\boldsymbol{w}_2$ were also estimated from the synthetic ECG (downsampled at 1000 Hz), using the algorithm described in [1]. In particular, at each beat, the iterative refinement was stopped when the correction, on each of the elements of $\boldsymbol{w}_1$ and $\boldsymbol{w}_2$, was smaller than 0.1%. An estimate of the $\mathcal{V}$-index ($\widetilde{\mathcal{V}}_i$) was derived using eq. (2).

3. Results

Using repolarization times $\rho_m(k)$ and delays $\Delta \rho_m(k)$, obtained from the simulations, we derived

$$\vartheta_m = \frac{1}{N} \sum_{k=1}^{N} \Delta \rho_m(k) \qquad \varphi_m(k) = \Delta \rho_m(k) - \vartheta_m,$$

where N is the number of beats. Only the last 200 beats of each run were considered, to avoid possible initial transients. Fluctuations in repolarization times $\varphi_m(k)$ were strongly correlated across nearby nodes, and σ_{φ_m} varied slightly in the slab (case 1B: $0.22 - 0.53$ ms). Table 1 contains a summary of the results. Values of σ_{φ_m} and $\mathcal{V}$, as reported, are averages across nodes and leads, respectively.

The three terms in eq. (4) were computed separately and are included in the table. Furthermore, for case 3, the metrics were re-evaluated considering only a subset of the 392 beats, with "stationary" RR. In particular, we
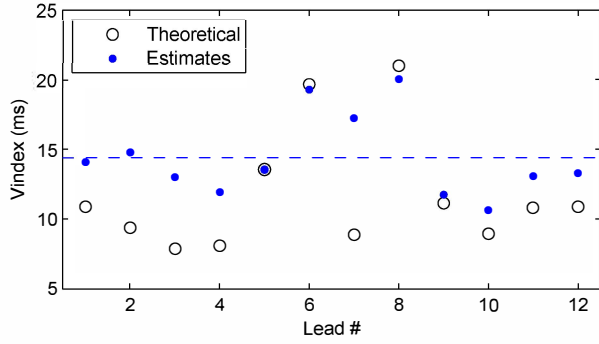
Figure 2. Values of $\mathcal{V}_i$ and $\widetilde{\mathcal{V}}_i$ for case 1B. The sketched line is the $\widetilde{\mathcal{V}}_i$ average values, also reported in table 1.

included only those beats having two proceeding RR intervals (RR_{k-1} and RR_{k-2}) within ± 25 ms the duration of the median RR. This latter case is termed "3*" in the table. Very similar results were obtained with different beat-selection strategies (results not reported). Summarizing, values for cases 3 and 3* were close as long as RR_{k-1} were similar across beats (the closer the better). The further similarity of RR_{k-2} improved the congruency, but only in a minor way. The threshold selected here (*i.e.* ± 25 ms) was a trade-off between stationarity and a sufficient number of beats, for statistical consistency.

The results described, so far, were obtained from the repolarization times of nodes in the slab only (and the two matrices **A**). Estimates of the $\mathcal{V}$-index ($\widetilde{\mathcal{V}}_i$) were also obtained from the synthetic ECG, as described in section 2.3. Values for case 1B are in fig. 2, while averages across leads are reported at the bottom of table 1.

4.   Conclusions and discussion

Theoretical values of $\mathcal{V}$ approximatively matched s_ϑ for case 1, even if a bias was present, as expected from [1] and eq. (4). In the other two cases, they largely underestimated it. When the temporal variability of $\Delta\boldsymbol{\rho}$ was driven only by RR variability (case 2), the value of $\mathcal{B}_2$ suggests that the excessive correlation within nodes (their temporal oscillations are more synchronized) hinders the estimate of s_ϑ from lead factors. The situation was only ameliorated when I_{Ks} stochastic gating was also included (case 3). However, in this last situation (closer to reality), the selection of a proper subset of stationary beats, removed the ambiguity (case 3*) and confirmed that the $\mathcal{V}$-index definition is well posed and of practical application.

Numerical estimates of $\widetilde{\mathcal{V}}_i$, from synthetic ECG, were substantially coherent with theoretical values $\mathcal{V}_i$, disregarding the numerical scheme employed to simulate them. The results suggest that the lead factors might be indeed estimated from surface ECG. The work partially overcome the limitations of assumption ii., hinting that the $\mathcal{V}$-index could be alternatively derived without using an ESS model.

Finally, the analysis of case 3* provided practical suggestions on which beats must be selected when analysing real ECG recordings and confirmed that only stationary ones need to be considered.

Acknowledgments

References

[1]   Sassi R, Mainardi LT. An estimate of the dispersion of repolarization times based on a biophysical model of the ECG. IEEE Trans Biomed Eng 2011;58:3396–3405.

[2]   van Oosterom A. Genesis of the T wave as based on an equivalent surface source model. J Electrocardiol 2001;34 Suppl:217–227.

[3]   Task Force of ESC and NASPE. Heart rate variability standards of measurement, physiological interpretation, and clinical use. Circulation 1996;93:1043–1065.

[4]   Sassi R, Mainardi LT. Quantification of spatial repolarization heterogeneity: Testing the robustness of a new technique. Comput Cardiol 2012;39:69–72.

[5]   Tung L. A bi-domain model for describing ischemic myocardial D-C potentials. Ph.D. thesis, Massachusetts Institute of Technology, 1978.

[6]   Heidenreich EA, Ferrero JM, Doblaré M, Rodríguez JF. Adaptive macro finite elements for the numerical solution of monodomain equations in cardiac electrophysiology. Ann Biomed Eng 2010;38:2331–2345.

[7]   ten Tusscher KHWJ, Panfilov AV. Alternans and spiral breakup in a human ventricular tissue model. Am J Physiol Heart Circ Physiol 2006;291:H1088–H1100.

[8]   Pueyo E, Corrias A, Virág L, Jost N, Szél T, Varró A, Szentandrássy N, Nánási P, Burrage K, Rodríguez B. A multiscale investigation of repolarization variability and its role in cardiac arrhythmogenesis. Biophys J 2011;101:2892–2902.

[9]   Min. cholé A, Pueyo E, Rodríguez J, Zacur E, Doblaré M, Laguna P. Quantification of restitution dispersion from the dynamic changes of the T-wave peak to end, measured at the surface ECG. IEEE Trans Biomed Eng 2011;58:1172–1182.

[10] Keller DUJ, Weber FM, Seemann G, Dossel O. Ranking the influence of tissue conductivities on forward-calculated ECGs. IEEE Trans Biomed Eng 2010;57:1568–1576.

Address for correspondence:

Roberto Sassi
Dipartimento di Informatica, Università degli Studi di Milano
via Bramante 65, 26013 Crema (CR) Italy
E-mail: roberto.sassi@unimi.it